Structural Implications of the Chemical Modification of Cys^{10} on Actin

Luba Eli-Berchoer,* Emil Reisler,† and Andras Muhlrad*†

*Department of Oral Biology, Hadassah School of Dental Medicine, Hebrew University, Jerusalem 91120, Israel, and †Department of Chemistry and Biochemistry, University of California, Los Angeles, California 90095 USA

ABSTRACT Cys^{10} is located in subdomain 1 of actin, which has an important role in the interaction of actin with myosin- and actin-binding proteins. Cys^{10} was modified with fluorescence probes *N*-(iodoacetyl)*N*′-(5-sulfo-1-naphthyl)ethylene diamine (IAEDANS), 7-diethylamino-3-(4′-maleimidylphenyl)-4-methylcoumarin (CPM), or monobromo bimane (MBB) by the method of Drewes and Faulstich (1991, *J. Biol. Chem.* 266:5508–5513). The specificity of Cys^{10} modification was verified by showing that the 33-kDa subtilisin fragment of actin (residues 48–375), which contains all of the actin thiols but Cys^{10}, is not fluorescent. Cys^{10} modification exposed a new site on actin to subtilisin cleavage. Edman degradation revealed this site to be between Ala^{19} and Gly^{20}. The modification slightly increased the rate of ϵATP-ATP exchange and decreased the rates of G-actin ATPase and polymerization. The activation of S1 ATPase by Cys^{10}-modified F-actin showed small probe-dependent changes in the values of V_{max} and K_M. The sliding speed of actin filaments in the in vitro motility assay remained unchanged upon modification of Cys^{10}. These results indicate that although the labeling of Cys^{10} perturbs the structure of subdomain 1, the modified actin remains fully functional. The binding of S1 to actin filaments decreases the accessibility of Cys^{10} probes to acrylamide and nitromethane quenchers. Because Cys^{10} does not participate directly in either actin polymerization or S1 binding, our results indicate that actin-actin and actin-myosin interactions induce dynamic, allosteric changes in actin structure.

INTRODUCTION

Actin is one of the most ubiquitous and abundant proteins in nature. It is one of the main constituents of the cell cytoskeleton, and its interaction with the myosin motor coupled with the hydrolysis of ATP is the molecular basis of muscle contraction. Actin exists in monomer (G) and polymer (F) forms. According to crystallographic data, the monomer of actin consists of four subdomains (Kabsch et al., 1990). As shown by limited proteolysis (Strzelecka-Golaszewska et al., 1993) and fluorescence labeling (Frieden et al., 1980; Frieden and Patane, 1985), the structure of G-actin is rather dynamic, and it changes upon Ca-Mg and ATP-ADP exchange. Normal mode analysis has also indicated significant movements of subdomains and loops in the actin structure (Tirion et al., 1995). Until now conformational changes in actin were studied primarily in its subdomain 2 and at the C-terminus because of their easy accessibility to proteases and chemical reagents (Frieden et al., 1980; Hegyi et al., 1974; Strzelecka-Golaszewska et al., 1993).

F-actin has been assumed to be a passive element in the myosin-powered cross-bridge cycle of contraction. Recently, however, the accumulating evidence about the dynamic nature of actin filaments (Drummond et al. 1990; Prochniewicz and Yanagida, 1990; Prochniewicz et al., 1996a; Orlova and Egelman, 1995; Orlova et al., 1995; Kim et al., 1998) has indicated an active role of actin in the molecular mechanism of muscle contraction. Several biochemical and structural studies have indicated that actin filament exists in different conformations, depending on bound cation, nucleotides, and proteins. It has been shown by image reconstruction of electron micrographs that a bridge of density, which has been suggested to arise from a major structural shift at the C-terminus, exists between the two strands of the actin filament in Ca-F-actin and is absent in Mg-F-actin (Orlova and Egelman, 1995). The nature of the tightly bound divalent cation and the addition of KCl influence the proteolytic susceptibility of F-actin at subdomain 2 and near the C-terminus (Strzelecka-Golaszewska et al., 1996). Phosphate (P_i) and its analogs, like beryllium fluoride, influence the three-dimensional structure of the filament (Orlova and Egelman, 1992) and, according to our results (Muhlrad et al., 1994), induce conformational changes in F-actin that are highly cooperative and extend over several monomers. A single gelsolin molecule nucleating a new filament affects in a cooperative manner the conformation of the whole actin filament (Orlova et al., 1995; Prochniewicz et al., 1996b). Myosin subfragment 1 (S1) has a significant effect on the structure of the actin filament: it increases the filament flexibility (Menetret et al., 1991) and rotational motion (Ng and Ludescher, 1994), immobilizes internal motion (Thomas et al., 1979), and decreases the distance between two domains of the actin monomer, resulting in a more compact molecule (Miki and Kouyama, 1994).

Despite the important role of subdomain 1 in actin in interactions with myosin and several actin-binding proteins, little is known about conformational changes that occur on it. This is due to the lack of an accessible residue that could be labeled with an environment sensitive probe. The finding

Received for publication 16 August 1999 and in final form 28 November 1999.

Address reprint requests to Dr. Andras Muhlrad, Department of Oral Biology, Hadassah School of Dental Medicine, Hebrew University, Jerusalem 91120, Israel. Tel.: 972-2-6757-587; Fax: 972-2-6784-010; E-mail: muhlrad@cc.huji.ac.il.

0006-3495/00/03/1482/08 $2.00

of Drewes and Faulstich (1991) that Cys^{10} on subdomain 1 can be selectively modified in Cys^{374}-blocked MgADP-G-actin appears to offer such a choice. We explored this possibility and labeled Cys^{10} with three different environment-sensitive fluorescent reagents. The specificity of the labeling and the effect of the modification of Cys^{10} on actin structure and function were examined in this work. The results show that while the modification perturbs the structure of subdomain 1, actin nevertheless remains fully functional after the labeling. Spectroscopic evidence is provided for conformational changes in the vicinity of Cys^{10} due to actin polymerization and the binding of S1. A preliminary report of this study was presented at a Biophysical Society Meeting (Eligula et al., 1998).

MATERIALS AND METHODS

Reagents

N-(Iodoacetyl)*N*′-(5-sulfo-1-naphthyl)ethylene diamine (IAEDANS), 7-diethylamino-3-(4′-maleimidylphenyl)-4-methylcoumarin (CPM), and monobromo bimane (MBB) were purchased from Molecular Probes (Eugene, OR). ATP, ADP, dithioerythritol (DTE), *N*-ethyl maleimide (NEM), subtilisin, and phenylmethylsulfonyl fluoride (PMSF) were from Sigma Chemical Co. (St. Louis, MO).

Proteins

Myosin and actin were prepared from rabbit back and leg muscles by the methods of Tonomura et al. (1966) and Spudich and Watt (1971), respectively. S1 and heavy meromyosin (HMM) were obtained by digestion of myosin filaments with chymotrypsin, following the procedures of Weeds and Taylor (1975) and Margossian and Lowey (1982), respectively. Protein concentrations were estimated from their absorption by using an $A^{1\%}$ at 280 nm of 7.5 cm^{-1} and 6.5 cm^{-1} for S1 and HMM, respectively, and an $A^{1\%}$ at 290 nm of 6.3 cm^{-1} for actin. Whenever appropriate, light scattering corrections were applied. Molecular masses were assumed to be 115, 350, and 42.3 kDa for S1, HMM, and actin monomers, respectively.

Chemical modification

Essentially, the procedure of Drewes and Faulstich (1991) was followed in the selective modification of Cys^{10}. CaATP-G-actin (100–120 μM) in G-buffer (0.1 mM $CaCl_2$, 0.2 mM ATP, 0.5 mM β-mercaptoethanol, 1.0 mM NaN_3, 1.0 mM $NaHCO_3$, pH 7.6) was incubated with 3.0 mM NEM on ice for 2 h to block Cys^{374}. The reaction was terminated by adding 3.0 mM DTE. The NEM-labeled actin was filtered through a Sephadex G-50 spin column equilibrated with 50 μM $MgCl_2$ and 5.0 mM Tris-HCl (pH 8.0). The filtered actin was polymerized by the addition of 0.2 mM EGTA and 2.0 mM $MgCl_2$ and incubation at room temperature for 30 min. F-actin was pelleted by centrifugation at 40,000 rpm at 4°C for 2 h and resuspended in 1.0 mM ADP, 50 μM $MgCl_2$, 5.0 mM Tris-HCl (pH 8.4). After overnight incubation on ice, actin was spin again at 40,000 rpm at 4°C for 2 h. The supernatant contained Cys^{374}-blocked MgADP-G-actin, which was modified at Cys^{10} with one of the three SH reagents, CPM, IAEDANS, or MBB. CPM, IAEDANS, and MBB were added in 1.5, 4.0, and 4.0 molar excesses over actin, respectively, and incubated on ice for 4 h. The reactions were terminated by adding 1.5 mM DTE and 0.5 mM ATP, and the actin was filtered through a Sephadex G-50 spin column equilibrated with 0.5 mM ATP, 50 μM $MgCl_2$, and 5.0 mM Tris-HCl at pH 7.8 (MgATP-G-actin buffer) to transform MgADP-G- to MgATP-G-actin. Actin was kept overnight in the MgATP-G-actin buffer before any further treatment to fully restore its structure (Drewes and Faulstich, 1991). The labeling stoichiometry of G-actin was determined spectrophotometrically by using the molar extinction coefficients of the three reagents (CPM $\epsilon_{384\ nm}$ = 16,450, IAEDANS $\epsilon_{336\ nm}$ = 5700, MBB $\epsilon_{396\ nm}$ = 5300). Actin labeling was 40–60% with IAEDANS, 60–90% with MBB, and ~100% with CPM. The concentrations of the Cys^{10}-labeled actins were calculated by taking into account the absorbance of the attached labels at 290 nm according to the following formulas:

$$\text{CPM-actin (mg/ml)} = (\text{O.D.}_{290} - 0.213 \times \text{O.D.}_{384})/0.63$$

$$\text{IAEDANS-actin (mg/ml)} = (\text{O.D.}_{290} - 0.313 \times \text{O.D.}_{336})/0.63$$

$$\text{MBB-actin (mg/ml)} = (\text{O.D.}_{290} - 0.38 \times \text{O.D.}_{396})/0.63$$

Subtilisin digestion

Labeled MgATP-G-actin and F-actin were digested with subtilisin at 1000:1 and 500:1 ratios (w/w) of actin to protease, respectively, at 25°C in the corresponding G- and F-buffers (1.0 mM $MgCl_2$, 20 mM Tris-HCl, pH 7.8). The digestion was terminated at different times with 1.0 mM PMSF and analyzed by sodium dodecyl sulfate-polyacrylamide gel electrophoresis (SDS-PAGE). N-terminal Edman sequence analysis was performed on subtilisin-cleaved, labeled F-actin.

Fluorescence measurements

All fluorescence measurements were made in a PTI spectrofluorometer (Photon Technology Industries Co., South Brunswick, NJ) at 25°C. Excitation wavelengths for CPM-, IAEDANS-, and MBB-labeled actins were set at 390, 334, and 380 nm, respectively.

Fluorescence quenching

Fluorescence quenching measurements were performed on labeled actin samples in 0.1 mM $MgCl_2$, 0.4 mM ATP, and 5.0 Tris-HCl (pH 7.8) at 25°C by adding nitromethane or acrylamide (in 5–40-μM consecutive steps) and averaging the fluorescence signal for 30 s. Emission wavelengths for CPM-, IAEDANS-, and MBB-labeled actin were set at 460, 485, and 475 nm, respectively (for excitation wavelengths see Fluorescence Measurements, above). Stern-Volmer constants (K_{SV}) were calculated from the plots of F_o/F (F_o and F, fluorescence intensities in the absence and presence of quencher, respectively) against quencher concentration.

ATP-ϵATP exchange

Labeled and unlabeled MgATP-G-actin (100 μM) was filtered through a Sephadex G-50 spin column equilibrated with 50 μM $MgCl_2$ and 5.0 mM Tris-HCl (pH 7.8). ϵATP was added at a 1.5-fold molar excess over filtered actin, and the sample was incubated on ice for 1 h. Immediately before the measurement, actin was diluted to 3.0 μM. The sample was transferred to a thermostatted spectrofluorometer cell (25°C), and the change in fluorescence was recorded after the addition of 200 μM ATP. Excitation and emission wavelengths were set at 340 nm and 410 nm, respectively.

Actin ATPase

Actin ATPase was assayed on labeled and unlabeled 10 μM MgATP-G-actin samples in 0.1 mM $MgCl_2$, 2.0 mM DTE, 0.4 mM ATP, 5.0 mM Tris-HCl (pH 7.6) at 25°C. At given time intervals 250-μl aliquots were withdrawn and the reaction was terminated by adding equal amounts of 0.6 M perchloric acid. Activity (micromoles of phosphate per micromole of

actin per hour) was calculated from the produced inorganic phosphate as measured by the malachite green dye method (Kodama et al., 1986).

Actin-activated S1 ATPase

Actin-activated S1ATPase activity (micromoles of phosphate per micromole of S1 per second) was calculated from the inorganic phosphate produced, measured according to the method of Fiske and Subbarow (1925). The reaction was carried out at 25°C on 1-ml aliquots taken at various time intervals. Incubation times were chosen such that no more than 15% of the ATP was hydrolyzed. The assay contained 0.1 μM S1 and between 2.5 and 40 μM F-actin in 2.0 mM $MgCl_2$, 20 mM HEPES buffer (pH 7.4), and 2.0 mM ATP. The ATPase data were fitted directly to the Michaelis-Menten equation to obtain the K_M and V_{max} values.

Actin polymerization

Polymerization of 10 μM MgATP-G-actin in 0.1 mM $MgCl_2$, 0.4 mM ATP, and 5.0 mM Tris-HCl (pH 7.8) was initiated by adding 2.0 mM $MgCl_2$. Polymerization was followed by light scattering at 25°C in a PTI spectrofluorometer. Both the excitation and emission wavelengths were set at 360 nm. Actin polymerization was also tested by pelleting the polymerized mixture at 75,000 rpm for 45 min in a Beckman TL-100 ultracentrifuge and subsequent analysis of the resulting pellet and supernatant by SDS-PAGE.

In vitro actin motility assay

This assay was performed at 25°C as described previously (Miller et al., 1996). HMM (300 μg/ml) was adsorbed to the nitrocellulose-coated coverslips. ATP-desensitized HMM was removed from the stock solution by pelleting HMM in the presence of actin and ATP. The assay solution was composed of 25 mM 3-(*N*-morpholino)propanesulfonic acid (pH 7.4), 25 mM KCl, 2.0 mM $MgCl_2$, 2.0 mM EGTA, 1.0 mM ATP, and the glucose-oxidase-catalase system to slow photobleaching. Methylcellulose (0.4%) was present in all solutions. Actin filaments were labeled by rhodamine phalloidin as described by Miller et al. (1996). Sliding speeds of actin filaments were determined using the Expertvision System (Motion Analysis, Santa Rosa, CA).

RESULTS

Specificity of Cys^{10} labeling and the perturbation of G-actin structure

Three fluorescent thiol reagents, CPM, IAEDANS, and MBB, were used for labeling Cys^{10} on Cys^{374}-blocked MgADP-actin. Because MgADP-G-actin easily undergoes spontaneous denaturation (Gershman et al., 1989), the labeled actin was transformed to the more stable MgATP-G-actin by incubating it in an excess of ATP for at least 12 h (Drewes and Faulstich, 1991). We verified, using both Cys^{374}-blocked G-actin that had been subjected to MgADP-MgATP transformation and control Cys^{374}-blocked MgATP-G-actin, that the above procedure of Cys^{10} labeling does not impair the main properties of actin, including polymerization, sedimentation, activation of myosin ATPase, and sliding of filaments in the in vitro motility assay. Thus, in accordance with Drewes and Faulstich (1991), we found that the incubation in MgATP-containing solution restores the native structure of MgATP-G-actin.

The specificity of Cys^{10} labeling was checked by subtilisin cleavage. Subtilisin cleaves G-actin between Met^{47} and Gly^{48} in the DNase 1 binding loop of subdomain 2. Of the two products of this cleavage, fragment 1–47 contains a single thiol, Cys^{10}, while the large C-terminal (48–375) fragment has the other actin thiols. In Fig. 1, *A* and *B*, are the electrophoretograms of MgATP-G-actin labeled with AEDANS on Cys^{10}, before and after subtilisin digestion. It can be seen that the undigested actin (Fig. 1 *A, lane a*) is highly fluorescent, while the 48–375 C-terminal proteolytic fragment, which is produced during the digestion (Fig. 1 *A, lanes b* and *c*) is not fluorescent (the small 1–47 fragment cannot be seen on the gel). The absence of a label on the 48–375 fragment, which contains the remaining actin thiols,

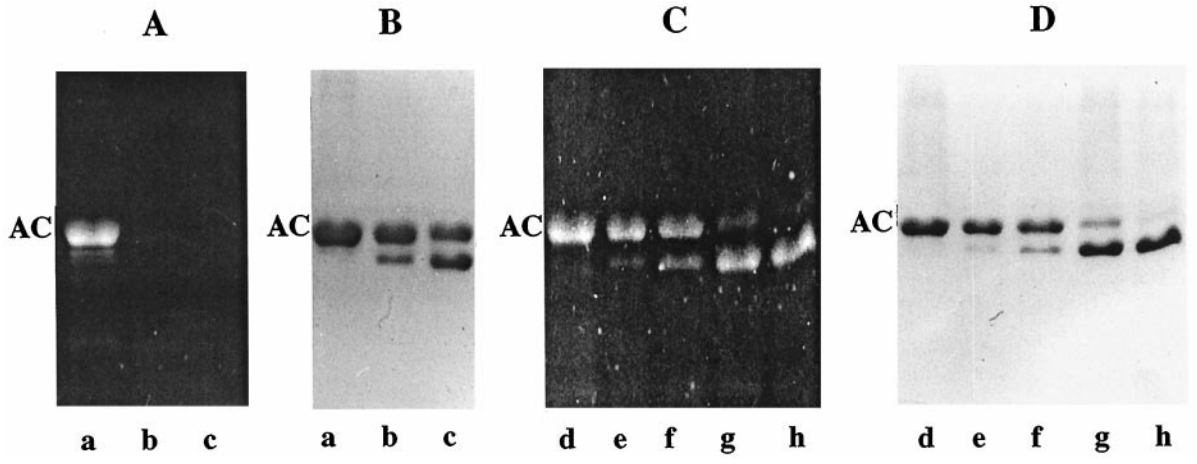

FIGURE 1 Subtilisin digestion of MgATP-G-actin labeled with IAEDANS on Cys^{10} or Cys^{374}. Actin was digested with subtilisin as described in Materials and Methods. (*A* and *B*) Cys^{10}-labeled actin. (*C* and *D*) Cys^{374}-labeled actin. *A* and *C* are fluorescent; *B* and *D* are Coomassie blue-stained electrophoretograms. *Lanes a* and *d*: Undigested actin; *lanes b, c, e–h*: actin digested for 5 min (*lanes b* and *e*), 10 min (*lanes c* and *f*), 30 min (*lane g*), and 60 min (*lane h*). Labeling stoichiometries for Cys^{10} and Cys^{374} labeling were 0.46 and 0.82 AEDANS/actin, respectively.

indicates that Cys^{10} has been selectively modified. As a control, Fig. 1 shows that after the subtilisin digestion of MgATP-G-actin labeled by AEDANS on Cys^{374}, both the intact actin and its 48–375 fragment are fluorescent (Fig. 1, *C* and *D*). Notably, in the Cys^{10}-labeled actin, fluorescence is absent not only in the C-terminal fragment but also in the upper, apparently undigested actin band (Fig. 1, *A* and *B*, *lanes b* and *c*). The loss of fluorescence from the "intact" actin band was also observed when AEDANS-Cys^{10}-F-actin, which is rather resistant to subtilisin digestion (Vahdat et al., 1995), was digested at a 500:1 (w/w) ratio of actin to subtilisin for 5 min (results not shown). The same loss of fluorescence was also observed with actin labeled with CPM and MBB (results not shown). We assumed that the fluorescence loss from the actin band is due to a cleavage in the N-terminal region of actin, which apparently does not influence the electrophoretic mobility of the protein. To test this assumption, N-terminal Edman degradation was performed on subtilisin-digested AEDANS-Cys^{10}-F-actin. Two sequences were obtained in the analysis. Because the N-terminus of actin is blocked, these sequences identify the locations of the subtilisin cuts. The major and minor sequences were Gly-Phe-Ala-Gly-Asp-Asp and Gly-Gln-Lys-Asp, respectively. The major sequence unambiguously assigns the location of the new subtilisin cleavage site to the region between Ala^{19} and Gly^{20}, near the N-terminus of actin. The minor sequence represents the known subtilisin cut between Met^{47} and Gly^{48} (Schwyter et al., 1989). The Ala^{19}-Gly^{20} site becomes available for subtilisin cleavage because of the perturbation of actin's structure by Cys^{10} labeling. This site is on a β-sheet that runs antiparallel relative to the β-sheet on which Cys^{10} is located (Fig. 2). The distance from the peptide bond between Ala^{19} and Gly^{20} to the sulfur atom of Cys^{10} is 6.5 Å (Kabsch et al., 1990).

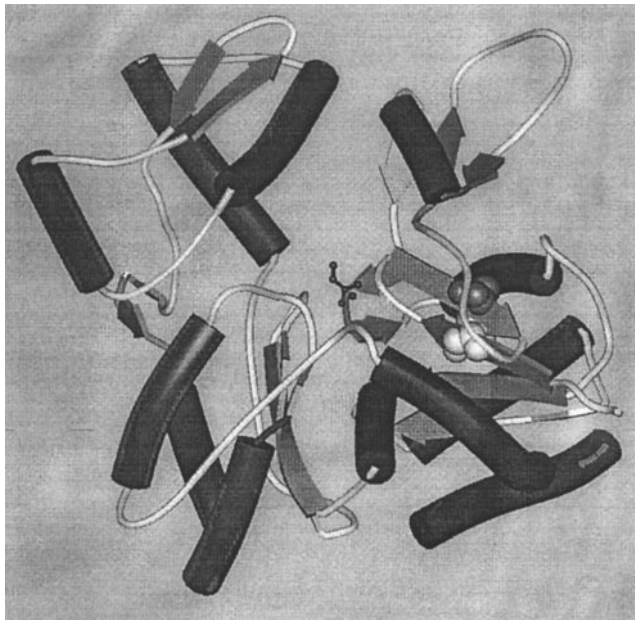

FIGURE 2 G-actin structure according to Kabsch et al. (1990). Full columns are α-helices, arrows are β-sheets. Light and dark spheres label Cys^{10} and Ala^{19}, respectively.

Energy transfer from tryptophans to fluorescent probes on Cys^{10}

Excitation of CPM-Cys^{10}-MgATP-G-actin at 297 nm produced two emission bands, a tryptophan band with a maximum at 330 nm and a CPM band with λ_{max} at 464 nm (Fig. 3 *A*). In comparison with the tryptophan emission of the unmodified MgATP-G-actin recorded under identical experimental conditions, the intensity of the tryptophan band of CPM-Cys^{10}-MgATP-G-actin is substantially decreased. This indicates fluorescence resonance energy transfer from the actin's tryptophans to the Cys^{10}-attached CPM probe. A decrease in fluorescence intensity of the tryptophan band relative to the unmodified MgATP-G-actin was also observed for AEDANS- and MBB-MgATP-G-actins (Fig. 3, *B* and *C*). According to the atomic structure of G-actin (Kabsch et al., 1990), the distances from the four actin tryptophans (79, 86, 340, and 356) to the sulfur atom of Cys^{10} are 12.0, 5.3, 6.9, and 11.6 Å, respectively. Because of the relatively short distances, all actin tryptophans may contribute to the observed energy transfer.

Characterization of Cys^{10}-modified actin

The ATPase activity of MgATP-G-actin was significantly decreased after Cys^{10} modification (Table 1). The larger decreases in ATPase were found with AEDANS- and MBB-modified actins, while the decrease with CPM-Cys^{10}-MgATP-G-actin was somewhat smaller. The rate of ϵATP-ATP exchange from MgϵATP-G-actin increased slightly as a result of the modification (Table 1). The order of the probe-dependent increase was AEDANS > CPM > MBB. These results support the conclusion derived from the appearance of a new subtilisin cleavage site, i.e., the modification of Cys^{10} causes some perturbations in the structure of actin.

The rates and extents of polymerization of Cys^{10}-labeled-MgATP-G-actins, measured by either light scattering or sedimentation, were similar to those of unmodified MgATP-G-actin (data not shown). The polymerized Cys^{10}-modified actins activated the Mg-modulated ATPase activity of S1 with only minor probe-dependent variations in the K_M and V_{max} values (Table 1). MBB-labeled F-actin activated S1 ATPase in a manner similar to that of its activation of native F-actin. The kinetic parameters of the ATPase activity were slightly affected when IAEDANS and CPM were used for modification (Table 1). In the in vitro motility assays no significant difference was found between the MBB-Cys^{10}-F-actin and unmodified F-actin filaments. The

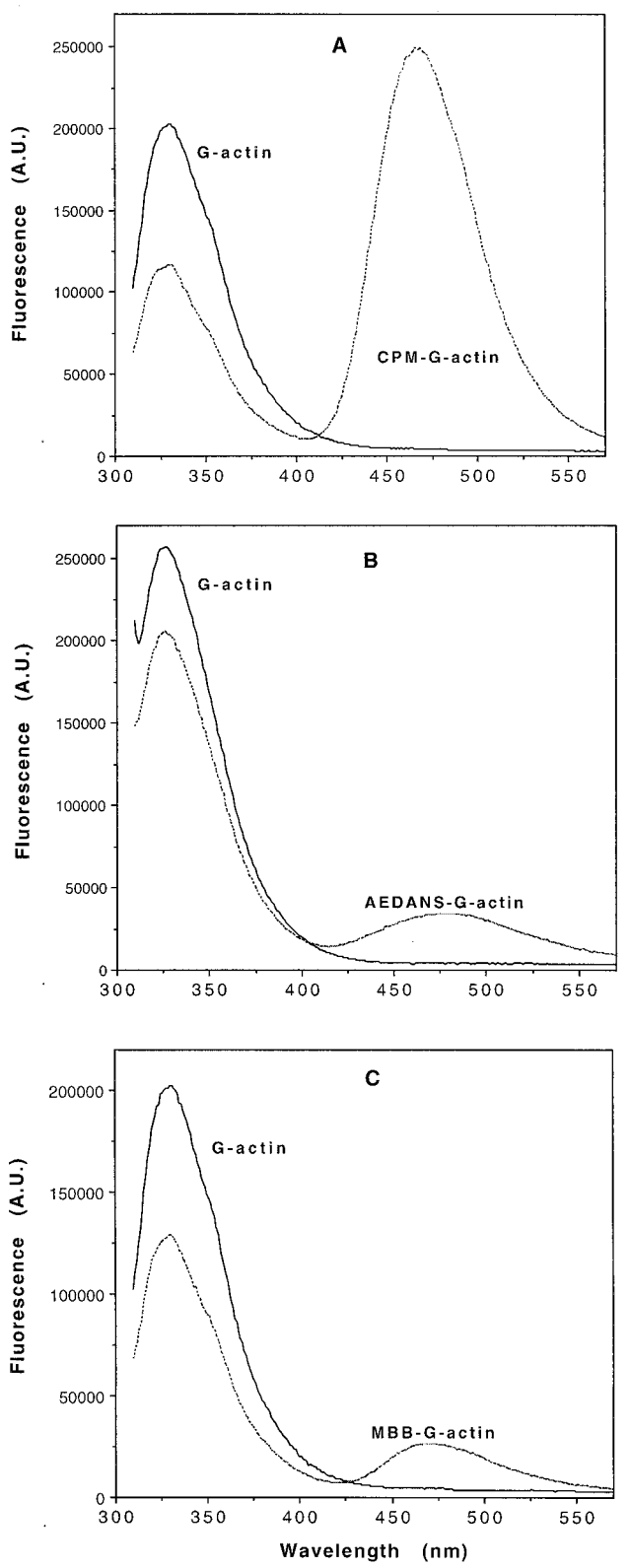

FIGURE 3 Emission spectra of MgATP-G-actin and Cys[10]-modified MgATP-G-actins excited at 297 nm. ——, G-actin; ·····, Cys[10]-labeled actins. (*A*) CPM-labeled; (*B*) AEDANS-labeled; (*C*) MBB-labeled G-actin. Labeling stoichiometries of CPM-, AEDANS-, and MBB-G-actin were 1.0, 0.41, and 0.9 probe/actin, respectively.

TABLE 1 Effect of modification of Cys[10] on nucleotide exchange and G-actin and acto-S1 ATPase

Cys[10] actin label	G-actin ATPase* (h^{-1})	$k_{exchange}$* (min^{-1})	Acto-S1 ATPase	
			K_M (μM)*	V_{max} (s^{-1})*
—	0.142 ± 0.016	0.49 ± 0.012	18.8 ± 1.2*	9.9 ± 0.8*
IAEDANS	0.083 ± 0.022	0.62 ± 0.014	17.4 ± 2.5	7.3 ± 0.2
CPM	0.101 ± 0.019	0.57 ± 0.021	25.8 ± 1.4	9.3 ± 0.7
MBB	0.087 ± 0.012	0.52 ± 0.009	18.3 ± 1.7	9.1 ± 0.4

ε-ATP-ATP exchange and G-actin and acto-S1 ATPase activities were measured as described in Materials and Methods. The rate constants (k) of the exchange reactions were calculated from plots fitted to single exponentials. The acto-S1 ATPase versus actin concentrations plots were fitted to a hyperbola, and the K_M and V_{max} values were calculated. Labeling stoichiometries of AEDANS-F-actin, CPM-F-actin, and MBB-F-actin were 0.56, 1.03, and 0.87 probe/actin, respectively.
*Mean ± SE of four independent experiments.

mean velocities for the control and the MBB-Cys[10]-F-actin filaments were 4.02 ± 0.81 and 4.03 ± 0.89 μm/s, respectively.

Effect of actin polymerization and S1 binding on the spectral characteristics of the Cys[10]-attached probes

Subdomain 1 of actin, where Cys[10] is located, has a key role in intermolecular interactions with actin and myosin. Therefore, it was of interest to examine the effect of actin polymerization and S1 binding on the Cys[10] environment. Fig. 4A shows the emission spectra of AEDANS-MgATP-Cys[10]-G-actin and F-actin recorded using an excitation at 297 nm. The intensity of the tryptophan band centered at 330 nm decreased, while the intensity on the AEDANS band, λ_{max} 486 nm, increased and blue shifted as a result of the polymerization. The tryptophan fluorescence decrease is comparable to that normally observed upon polymerization of unlabeled actin (Selden et al., 1994). The increase in the AEDANS band could be detected also upon direct excitation of the probe at the λ_{max} wavelength for its absorption (Fig. 4 *B*). In addition, the emission spectrum of AEDANS-Cys[10]-F-actin (Fig. 4 *B*) was blue shifted (λ_{max} 479 nm) relative to the spectrum of G-actin (λ_{max} 484 nm). Thus, the results shown in Figs. 4A and 4B indicate conformational changes in the vicinity of Cys[10] but not alterations in the fluorescence energy transfer between actin tryptophans and Cys[10]-AEDANS following actin polymerization. The fluorescence intensity of the MBB and CPM probes attached to Cys[10] decreased following the polymerization of actin (Fig. 4 C and D). These results support the conclusion about conformational changes that take place in the vicinity of Cys[10] during actin polymerization. Binding of S1 also affects the actin structure as manifested in the intensity decrease of the emission spectra of all probes attached to Cys[10] on F-actin (Fig. 4).

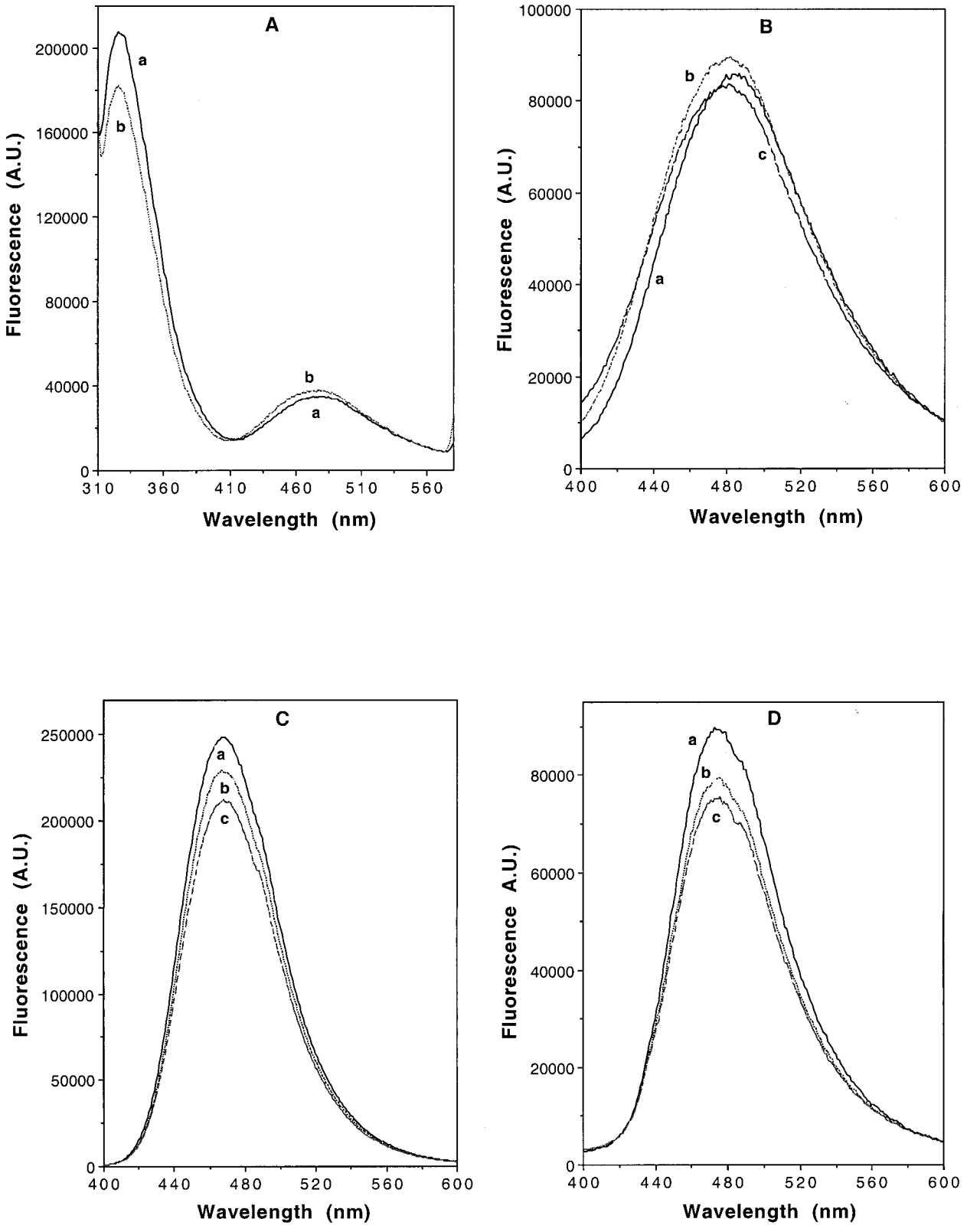

FIGURE 4 Effect of polymerization and S1 on the emission spectra of Cys^{10}-labeled MgATP-G-actins. (*A*) Emission spectra for AEDANS-labeled MgATP-G-actin and F-actin excited at 297 nm. (*B–D*) AEDANS- (*B*), CPM- (*C*), and MBB-actin (*D*) with excitation set at 334, 390, and 380 nm, respectively. Spectra: *a*, G-actin; *b,* F-actin; *c,* F-actin plus S1. For conditions of the measurements see Materials and Methods. Labeling stoichiometries of AEDANS-, CPM-, and MBB-actin were 0.51, 0.98, and 0.91 probe/actin, respectively.

The effect of polymerization and S1 binding on the accessibility of the probes on Cys^{10} was studied by collisional quenching of fluorescence with nitromethane and acrylamide (Table 2). Nitromethane quenches the fluorescence of all three probes while acrylamide is an effective quencher only for IAEDANS and CPM. The Stern-Volmer quenching constants (K_{SV}) were calculated by plotting F_o/F against the quencher concentration as described in MATERIALS AND METHODS. All plots were linear indicating the dynamic nature of the quenching. The probes on Cys^{10} are all partially shielded from the quenchers since their K_{SV} values are substantially smaller than those of free probes. The K_{SV} values obtained for F-actin were lower than those for G-actin but not for all combinations of probes and quenchers. On the other hand, addition of S1 significantly reduced the accessibility of probes to quenchers in all cases except the acrylamide quenching of AEDANS-Cys^{10}-F-actin. The quenching results substantiate the conclusion that actin polymerization and the binding of S1 induce conformational changes in the vicinity of Cys^{10} on subdomain 1 of actin.

DISCUSSION

Because of its reactivity and accessibility to reagents Cys^{374} on the actin C-terminus has been the main site for attachment of fluorescent and spin probes on α-actin. Other sites of actin labeling, Lys-61 and Tyr-69, although useful for fluorescence energy transfer (FRET) measurements (Barden et al., 1987; Miki et al., 1992), are involved in actin polymerization (Miki, 1987; Holmes et al., 1990; Chantler and Gratzer, 1975) and their derivatization affects actin properties. The labeling of Gln-41 on actin with a dansyl probe appears to have no effect on actomyosin interactions (Kim et al., 1998), but the transglutaminase mediated reaction does not offer the same labeling flexibility and choices as cysteine modifications do. These considerations prompted the attempts to label Cys^{10} on actin with reporter groups for spectroscopic studies. Specific modification of this residue appeared to be achieved on Cys^{374} pre-blocked G-actin in the presence of 2.0 M urea (Barden et al., 1987). However, the distances determined by FRET between Cys^{10} and other sites of actin were inconsistent with the atomic structure of G-actin suggesting that the exposure to urea might have altered its structure irreversibly (O'Donoghue et al., 1992). An alternative procedure for attacking Cys^{10} in the structurally labile MgADP-G-actin (with a pre-blocked Cys^{374}) was developed by Drewes and Faulstich (1991). According to these authors, the restoration of native G-actin structure is achieved upon transformation of the labeled MgADP-G-actin into MgATP-actin, following its long incubation with ATP.

The results of this study, with three different thiol regents, confirm the previous observation on the feasibility of a specific Cys^{10} modification and the reversal of the ADP-induced structural destabilization of actin (Drewes and Faulstich, 1991). Moreover this work documents that three key functional properties of actin are affected only marginally by, CPM, MBB, and AEDANS probes attached to Cys^{10}. The polymerization of labeled actin, its in vitro motility over HMM, and the kinetic parameters V_{max} and K_M of acto-S1 ATPase are similar to those of control actin. Obviously, our results show also that the fluorescent probes attached to Cys^{10} do induce probe-dependent, local changes in the nucleotide cleft and in loop 18–29. Importantly, these structural perturbations of actin by Cys^{10} probes have little impact on its polymerization and interactions with myosin. This indicates that the local perturbations caused by Cys-labeling either do not spread to functionally important sites on actin or are inconsequential to their action. Conversely, both polymerization of actin and the binding of S1 do cause small but distinct changes in the fluorescence emission of the probes. Because Cys^{10} is not located at the binding interface with S1 or with other actin protomers in F-actin, the above spectral transitions reflect allosteric changes in the environment of the probe, which are transmitted from other sites on actin. Thus, the main result of this study is the addition of the Cys^{10} site to the growing number of structural elements of actin that show dynamic changes upon S1 binding and actin-actin interaction. On the basis of the tests

TABLE 2 Quenching of fluorescent probes attached to Cys^{10} on actin

		Stern-Volmer constants (K_{SV})*			
Probe	Quencher	G-actin	F-actin	F-actin +S1	Free probe +Cys
IAEDANS	Nitromethane	28 ± 1.65	23.4 ± 1.35	18.9 ± 1.1	51.5 ± 0.21
CPM	Nitromethane	5.20 ± 0.09	5.40 ± 0.11	4.58 ± 0.05	9.3 ± 0.06
MBB	Nitromethane	2.11 ± 0.08	1.88 ± 0.08	1.53 ± 0.04	2.52 ± 0.03
IAEDANS	Acrylamide	3.60 ± 0.19	3.62 ± 0.45	3.04 ± 0.12	8.83 ± 0.11
CPM	Acrylamide	4.54 ± 0.25	3.76 ± 0.33	2.99 ± 0.19	ND

Stern-Volmer constants were calculated from plotting F_o/F (F_o and F are the fluorescence in the absence and presence of quencher, respectively) against quencher concentration as described in Materials and Methods. All plots were linear, indicating the dynamic nature of the quenching. Mean stoichiometries of labeling for AEDANS-, CPM-, and MBB-actin were 0.52, 0.98, and 0.93 probe/actin, respectively.
*Mean of four independent experiments ± SE.

carried out in this work, Cys^{10} probes should provide appropriate spectroscopic tool for monitoring such dynamic changes in actin via FRET measurements.

Supported by USPHS AR 22031 and NSF MCB-9630997 grants (to ER).

REFERENCES

Barden, J. A., and C. G. Dos Remedios. 1987. Fluorescence resonance energy transfer between sites in G-actin. The spatial relationship between Cys-10, Tyr-69, Cys-374, the high affinity metal and the nucleotide. *Eur. J. Biochem.* 168:103–109.

Chantler, P., and W. B. Gratzer. 1975. Effects of specific chemical modification of actin. *Eur. J. Biochem.* 60:67–72.

Drewes, G., and H. Faulstich. 1991. A reversible conformational transition in muscle actin is caused by nucleotide exchange and uncovers cysteine in position 10. *J. Biol. Chem.* 266:5508–5513.

Drummond, D. R., M. Peckham, J. C. Sparrow, and D. C. S. White. 1990. Alteration in crossbridge kinetics caused by mutations in actin. *Nature.* 348:440–442.

Eligula, L., E. Reisler, and A. Muhlrad. 1998. Chemical modification of Cys-10 on actin: structural and functional implications. *Biophys. J.* 74:A47.

Fiske, C. H., and Y. Subbarow. 1925. The colorimetric determination of phosphorus. *J. Biol. Chem.* 66:375–400.

Frieden, C., D. Lieberman, and H. R. Gilbert. 1980. A fluorescent probe for conformational changes in skeletal muscle G-actin. *J. Biol. Chem.* 255: 8991–8993.

Frieden, C., and K. Patane. 1985. Differences in G-actin containing bound ATP or ADP: the Mg^{2+}-induced conformational change requires ATP. *Biochemistry.* 24:4192–4196.

Gershman, L. C., L. A. Selden, H. J. Kinosian, and J. E. Estes. 1989. Preparation and polymerization properties of monomeric ADP-actin. *Biochim. Biophys. Acta.* 995:109–115.

Hegyi, G., G. Premecz, B. Sain, and A. Muhlrad. 1974. Selective carbethoxylation of the histidine residues of actin by diethylpyrocarbonate. *Eur. J. Biochem.* 44:7–12.

Holmes, K. C., D. Popp, W. Gebhard, and W. Kabsch. 1990. Atomic model of the actin filament. *Nature.* 347:44–49.

Kabsch, W., H.-G. Mannherz, D. Suck, E. Pai, and K. C. Holmes. 1990. Atomic structure of the actin:DNase I complex. *Nature.* 347:37–44.

Kim, E., E. Bobkova, C. J. Miller, A. Orlova, G. Hegyi, E. H. Egelman, A. Muhlrad, and E. Reisler. 1998. Intrastand cross-linked actin between Gln-41 and Cys-374. III. Inhibition of motion and force generation with myosin. *Biochemistry.* 37:17801–17809.

Kodama, T., K. Fukui, and K. Kometani. 1986. The initial phosphate burst in ATP hydrolysis by myosin and subfragment-1 as studied by a modified malachite green method for determination of inorganic phosphate. *J. Biochem. (Tokyo).* 99:1465–1472.

Margossian, S. S., and S. Lowey. 1982. Preparation of myosin and its subfragments from rabbit skeletal muscle. *Methods Enzymol.* 85:55–71.

Menetret, J. F., W. Hofman, R. R. Schhroder, G. Rapp, and R. S. Goody. 1991. Time-resolved cryo-electron microscopic study of the dissociation of actomyosin induced by photolysis of photolabile nucleotides. *J. Mol. Biol.* 219:139–144.

Miki, M. 1987. The recovery of the polymerization of Lys-61-labeled actin by the addition of phalloidin. *Eur. J. Biochem.* 164:229–235.

Miki, M., and T. Kouyama. 1994. Domain motion in actin observed by fluorescence resonance energy transfer. *Biochemistry.* 33:10171–10177.

Miki, M., S. I. O'Donoghue, and C. G. Dos Remedios. 1992. Structure of actin observed by fluorescence energy transfer spectroscopy. *J. Muscle Res. Cell Motil.* 13:132–145.

Miller, C. J., W. W. Wong, E. Bobkova, P. A. Rubenstein, and E. Reisler. 1996. Mutational analysis of the role of the N-terminus of actin in actomyosin interactions. Comparison with other mutant actins and implications for the cross-bridge cycle. *Biochemistry.* 35:16557–16565.

Muhlrad, A., P. Cheung, B. C. Phan, C. Miller, and E. Reisler. 1994. Dynamic properties of actin: structural changes induced by beryllium fluoride. *J. Biol. Chem.* 269:11852–11858.

Ng, C., and R. D. Ludescher. 1994. Microsecond rotational dynamics of F-actin in acto-S1 filaments during ATP hydrolysis. *Biochemistry.* 33: 9098–9104.

O'Donoghue, S. I., B. D. Hambly, and C. G. Dos Remedios. 1992. Models of actin monomer and filament from fluorescence resonance energy transfer. *Eur. J. Biochem.* 205:591–601.

Orlova, A., and E. H. Egelman. 1992. The structural basis for the destabilization of F-actin by phosphate release following ATP hydrolysis. *J. Mol. Biol.* 227:1043–1053.

Orlova, A., and E. H. Egelman. 1995. Structural dynamics of F-actin. I. Changes in the C-terminus. *J. Mol. Biol.* 245:582–797.

Orlova, A., E. Prochniewicz, and E. H. Egelman. 1995. Structural dynamics of F-actin. II. Cooperativity in structural transitions. *J. Mol. Biol.* 245:598–607.

Prochniewicz, E., and T. Yanagida. 1990. Inhibition of sliding movement of F-actin by cross-linking emphasizes the role of actin structure in the mechanism of motility. *J. Mol Biol.* 216:761–772.

Prochniewicz, E., Q. Zhang, E. C. Howard, and D. D. Thomas. 1996a. Microsecond rotational dynamics of actin: spectroscopic detection and theoretical simulation. *J. Mol. Biol.* 255:446–457.

Prochniewicz, E., Q. Zhang, P. A. Janmey, and D. D. Thomas. 1996b. Cooperativity in F-actin: binding of gelsolin at the barbed end affects structure and dynamics of the whole filament. *J. Mol. Biol.* 260: 756–766.

Schwyter, D., M. Phillips, and E. Reisler. 1989. Subtilisin-cleaved actin: polymerization and interaction with myosin subfragment 1. *Biochemistry.* 28:5889–5895.

Selden, L. A., H. J. Kinosian, J. E. Estes, and L. C. Gershman. 1994. Influence of the high affinity divalent cation on actin tryptophan fluorescence. *Adv. Exp. Med. Biol.* 358:51–57.

Spudich, J. A., and S. Watt. 1971. Regulation of rabbit skeletal muscle contraction. 1. Biochemical studies of interaction of tropomyosin-troponin complex with actin and proteolytic fragments of myosin. *J. Biol. Chem.* 246:4866–4871.

Strzelecka-Golaszewska, H., J. Moraczewska, S. Y. Khaitlina, and M. Mossakowska. 1993. Localization of the tightly bound divalent-cation-dependent and nucleotide-dependent conformation changes in G-actin using limited proteolytic digestion. *Eur. J. Biochem.* 211:731–742.

Strzelecka-Golaszewska, H., A. Wozniak, T. Hult, and U. Lindberg. 1996. Effects of the type of divalent cation, Ca^{2+} or Mg^{2+}, bound at high-affinity site and of the ionic composition of the solution on the structure of F-actin. *Biochem. J.* 316:713–721.

Thomas, D. D., J. C. Seidel, and J. Gergely. 1979. Rotational dynamics of spin labeled F-actin in the sub-millisecond time range. *J. Mol. Biol.* 132:257–273.

Tirion, M. M., D. Ben-Avraham, M. Lopez, and K. C. Holmes. 1995. Normal modes as refinement parameters for the F-actin model. *Biophys. J.* 68:5–12.

Tonomura, Y., P. Appel, and M. F. Morales. 1966. On the molecular weight of myosin. *Biochemistry.* 5:515–521.

Vahdat, A., C. Miller, M. Phillips, A. Muhlrad, and E. Reisler. 1995. A novel 27/16 form of subtilisin cleaved actin: structural and functional consequences of cleavage between Ser-234 and Ser-235. *FEBS Lett.* 365:149–151.

Weeds, A. G., and R. S. Taylor. 1975. Separation of subfragment-1 isoenzymes from rabbit skeletal muscle. *Nature.* 257:54–56.